MEASUREMENT OF THE TOTAL CROSS SECTION FOR THE $^1H(n, \gamma)^2H$ REACTION BETWEEN 37 AND 72 MeV ☆

M. BOSMAN [1], A. BOL [1], J.F. GILOT [2], P. LELEUX [3], P. LIPNIK [3] and P. MACQ

Institut de Physique Corpusculaire, Université Catholique de Louvain, B-1348 Louvain-la-Neuve, Belgium

Received 9 January 1979

The total cross section for radiative neutron–proton capture has been measured at 37, 42, 47, 52, 63 and 73 MeV. The inverse process, the photodisintegration of the deuteron, was measured in the same energy range by different authors with contradictory results, some of them in large disagreement with all theoretical predictions of the cross section. The submitted data are in agreement with theory and the results of a recent total absorption experiment.

Radiative neutron–proton capture is one of the elementary electromagnetic processes in nucleon–nucleon interaction. The inverse reaction, deuteron photodisintegration, has been studied widely in the last few years but there exist, in the photon energy range of 15 to 40 MeV, large discrepancies between the data reported by different groups [1–5] and theoretical predictions. The main object of the present work is to disentangle this controversy by a new experimental approach, i.e. the direct measurement of the n–p capture cross section between 37 and 72 MeV neutron energy, which corresponds to E_γ = 21–38 MeV.

The salient features of the experimental method are: (1) The deuterons from n–p capture are detected in a compact set-up mounted along the incident neutron beam; note that the whole (0° to 180° c.m.) angular range of the deuteron is constrained in the laboratory system to a narrow forward cone of less than ± 7° opening angle. (ii) Simultaneously, i.e. for the same neutron flux and target thickness, the protons elastically scattered at 3.3° laboratory angle are counted in a solid angle $\Delta\Omega$. (iii) The n–p capture total cross section (σ_c) is inferred from the number of detected deuterons (N_d) and protons (N_p) by means of $\sigma_c = (N_d/N_p)\mathrm{d}\sigma/\mathrm{d}\Omega(173^\circ \text{ c.m.}) J\Delta\Omega$, where $\mathrm{d}\sigma/\mathrm{d}\Omega$ (173° c.m.), the differential n–p scattering cross section, is extracted from elastic scattering data, and J is the solid angle jacobian.

The experimental set-up is represented in fig. 1. The neutron beam has been described in detail [6]; a 3 μA proton beam of 40, 50, 55, 60, 65, and 75 MeV from the Louvain-la-Neuve isochronouscyclotron (CYCLONE) bombards a 4 mm thick lithium target. The produced neutrons are collimated to define a 3 cm beam diameter at 3 m from the production target. Events from charged particles contaminating the neutron beam ($\approx 10^{-4}$) are rejected by a first gas proportional counter (PC1, placed in front of the liquid hydrogen target. This target, 4.5 or 6.5 mm thick and 4 cm in diameter, is located at 3 m downstream the neutron production target. The neutrons cross the hydrogen volume and its vacuum jacket, through thin Havar windows (5 mg/cm^2 and 10 mg/cm^2, respectively). Behind the target, a second proportional counter (PC2), 2 cm thick, triggers on charged particles from the target region. Both proportional counters are filled with an isobutane–methylal–argon mixture confined by 5 mg/cm^2 Havar and 2.7 mg/cm^2 aluminium windows, respectively.

The energy of the incident neutrons from the Li(p, n) reaction is selected by a measurement of the time-of-flight (TOF) between a capacitive beam time

☆ Work supported by IISN (Institut Interuniversitaire des Sciences Nucléaires); in partial fulfilment of M.B. Ph. D. Thesis.

[1] Chercheur agréé of IISN.

[2] Boursier IRSIA.

[3] Chercheur FNRS.

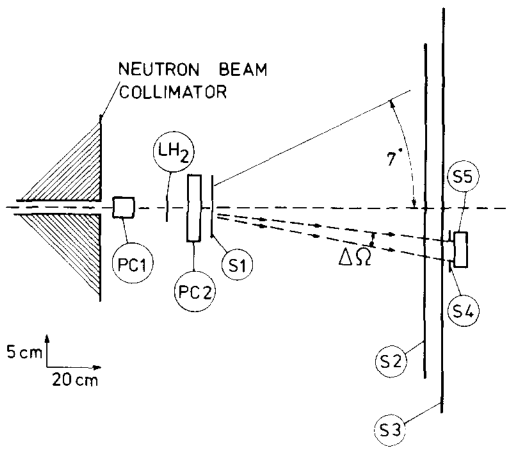

Fig. 1. Experimental set-up. The direction of the neutron beam is represented by the central dashed line; $\Delta\Omega$ is the solid angle for proton detection. Other symbols are defined in the text.

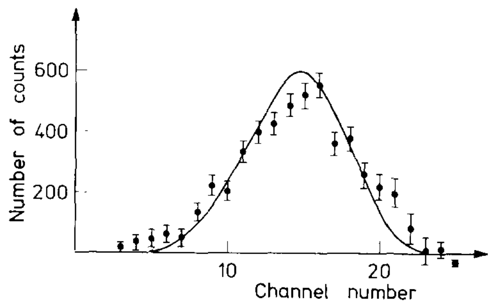

Fig. 2. Deuteron energy spectrum obtained at E_n = 52.4 MeV as the difference of runs with hydrogen target and dummy target. The curve represents the deuteron spectrum calculated from the kinematical energy distribution of the capture process taking into account the deuteron energy losses and the experimental scintillator response function.

pick-off in front of the Li target and the scintillator S1, S1 is a thin (0.1 or 0.5 mm) ΔE scintillator; S2 intercepts all the deuterons from n–p capture and its thickness is adjusted to their maximum range; multiple scattering is reduced by a helium bag placed between S1 and S2. The scintillator S3 (2 mm thick), is slightly larger than S2 and just behind it. Protons from backward n–p elastic scattering are detected by scintillator S5, 5 cm thick and 5 cm diameter, situated at a laboratory angle of 3.3°; the solid angle of S5 is defined by a 3 cm diameter hole in scintillator S4. The signature for fast protons is thus the combination: $\overline{\mathrm{PC1}}$ PC2 S1 S2 S3 $\overline{\mathrm{S4}}$ S5 and for deuterons or slow protons stopped in S2: $\overline{\mathrm{PC1}}$ PC2 S1 S2 $\overline{\mathrm{S3}}$. Such a signal triggers the recording of an event i.e.: (i) the kind of combination, (ii) all the pulse heights ΔE or E from the gas or scintillation counters and (iii) three TOF signals between S1 and the beam pick-off, S1 and S2, S1 and S5. This information is stored on magnetic tape via a CAMAC system linked to a PDP 11-20 computer. Runs taken are alternately with the filled hydrogen target and an empty one.

The best mass separation of the stopped particles in S2, i.e. between deuterons and slow protons, is obtained from the biparametric spectrum of the S2 pulse height and the TOF between S1 and S2. With a selection of the fast neutron peak from Li(p, n), the signal-to-background ratio in the region of the deuteron mass is about 1/4. Fig. 2 represents a typical deuteron energy spectrum obtained from the difference of the results with filled and empty hydrogen target at E_n = 52.4 MeV.

Final results are summarized in table 1 and fig. 3. Error bars represent the consistency error taken over successive pairs of measurements with hydrogen and dummy target. The 173° c.m. n–p elastic differential cross section, through which our data are normalized, is taken from a fit of all experimental data [7] between 22 and 80 MeV incident neutron energy. These data and the results obtained from a local-energy phase-shift analysis of n–p and p–p data around 50 MeV [8], are in agreement within ± 5%.

Photodisintegration data are generally compared to the non-relativistic phenomenological treatment of Partovi [9] using the Hamada–Johnston potential. Recently the Low theorem was applied to a relativistic evaluation of the process, with the following parameters for the nuclear interaction: the deuteron binding energy and the neutron–proton triplet effective range. The two theoretical approaches are consistent in the E_γ = 20 to 40 MeV region, the second one suggesting a new way to extract the triplet effective range from a coherent set of photodisintegration data [10].

There are two recent measurements of the photodisintegration cross section, one between 17 and 25 MeV photon energy [4], the other between 25 and

Table 1
Experimental results for the n–p radiative capture cross section with the c.m. value of the differential elastic cross section at 173° used for normalization. The two last columns translate the present results, by application of detailed balance, into the corresponding photodisintegration energy and cross section.

E_n (MeV)	$\sigma_{capture}$ (μb)	$d\sigma/d\Omega(173°)$ (mb/sr)	E_γ(MeV) corresponding to E_n	$\sigma_{photodisintegration}$ (μb)
37.0 ± 1.4	21.2 ± 1.6	23.2	20.8	582 ± 44
42.2 ± 1.3	20.6 ± 1.4	20.4	23.4	511 ± 35
47.3 ± 1.2	17.0 ± 0.7	18.2	25.9	385 ± 16
52.4 ± 1.1	17.6 ± 0.9	16.7	28.5	367 ± 19
57.4 ± 1.0	15.8 ± 1.1	15.4	31.0	306 ± 21
62.5 ± 1.0	14.6 ± 1.1	14.4	33.5	264 ± 20
72.6 ± 0.9	14.7 ± 1.1	12.8	38.6	234 ± 18

43 MeV [3]. Such experiments have to rely on an absolute measurement of the target thickness and of the photon flux produced from a hardened bremsstrahlung spectrum. They are also based on a knowledge of the theoretical form of the differential cross section. The discrepancy with the theory amounts to 20% at 20 MeV proton (40 MeV neutron) energy. This discrepancy triggered a new measurement [5] performed between 15 and 25 MeV, in which an original total absorption measurement of the photon flux in D_2O and H_2O targets with a Compton spectrometer as photon detector has been used. Therefore, this result is independent of the photon flux and target thickness, but the experiment, dominated by atomic cross sections, is very sensitive to photon absorption differences between H_2O and D_2O.

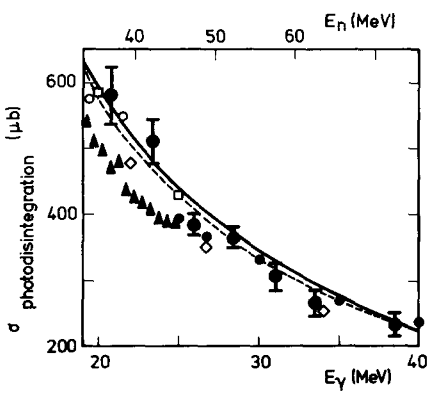

Fig. 3. Experimental cross section measured in the present experiment (•) compared, by means of the detailed-balance theorem, to photodisintegration data of ref. [1] (◇), ref. [2] (○), ref. [3] (○), ref. [4] (▲) and ref. [5] (□). The error bars do not include systematic errors from the normalization (± 5%). The continuous line represents Partovi's calculation [9], and the dashed one the results from the Low-theorem approach with the triplet effective range value r_{0t} = 1.70 fm. The horizontal scales show either the neutron (E_n) or the corresponding γ-ray (E_γ) energy in the laboratory system.

The present measurements are also free from uncertainties in the neutron flux and hydrogen target thickness, but a critical point remains the normalization to the n–p differential cross section, which is only known with a precision of ± 5%.

In conclusion, the last two reported experiments, with systematic errors of quite different origin, tend to show that there is no anomaly between experiment and theory for this elementary process in the investigated energy range.

We wish to thank the workshop and cyclotron teams for their careful work, Dr. R.A. Arndt for sending us data and details about the phase-shift analysis, and Prof. M.J. Moravcsik, Drs. B. Ziegler, J. Ahrens and A. Zieger for many comments.

References

[1] L. Allen, Phys. Rev. 98 (1955) 705.
[2] A. Whetstone and J. Halpern, Phys. Rev. 109 (1958) 2072.
[3] B. Weissman and H.L. Schultz, Nucl. Phys. A174 (1971) 129.
[4] J.E.E. Baglin, R.W. Carr, E.J. Bentz and C.P. Wu, Nucl. Phys. A201 (1973) 593.
[5] J. Ahrens et al., Phys. Lett. 52B (1974) 49.
[6] M. Bosman et al., Nucl. Instr. Meth. 148 (1978) 363.
[7] E.R. Flynn and P.J. Bendt, Phys. Rev. 128 (1962) 1268; T.C. Montgomery et al., Phys. Rev. C16 (1977) 499;

M.J. Saltmarsh et al., Oak Ridge National Laboratory, unpublished; these data are extracted from R.A. Arndt, J. Binstock and R. Bryan, Phys. Rev. D8 (1973) 1397.
[8] R.A. Arndt, R.H. Haekman and L.D. Roper, Phys. Rev. C15 (1977) 1021 and earlier communications.
[9] F. Partovi, Ann. Phys. 27 (1964) 79.
[10] J.L. Lucio, A. Martínez and J. Pestieau, private communication.